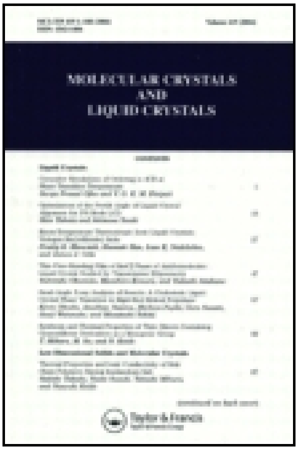

Molecular Crystals and Liquid Crystals
Publication details, including instructions for authors and subscription information:
http://www.tandfonline.com/loi/gmcl20

Ion Beam Alignment of Nematic Liquid Crystal on MEH-PPV-Layers

S. Pylypenko [a], K. Artyushkova [a], J. E. Fulghum [a], O. Buluy [b], N. Aryasova [b] & Yu. Reznikov [b]

[a] The University of New Mexico, Farris Engineering Center, Albuquerque, New Mexico, USA

[b] Institute of Physics of National Academy of Science, Prospect Nauki, Kyiv, Ukraine

Version of record first published: 22 Sep 2006

To cite this article: S. Pylypenko, K. Artyushkova, J. E. Fulghum, O. Buluy, N. Aryasova & Yu. Reznikov (2006): Ion Beam Alignment of Nematic Liquid Crystal on MEH-PPV-Layers, Molecular Crystals and Liquid Crystals, 454:1, 167/[569]-177/[579]

To link to this article: http://dx.doi.org/10.1080/15421400600654066

Mol. Cryst. Liq. Cryst., Vol. 454, pp. 167/[569]–177/[579], 2006
Copyright © Taylor & Francis Group, LLC
ISSN: 1542-1406 print/1563-5287 online
DOI: 10.1080/15421400600654066

Ion Beam Alignment of Nematic Liquid Crystal on MEH-PPV-Layers

S. Pylypenko
K. Artyushkova
J. E. Fulghum
The University of New Mexico, Farris Engineering Center,
Albuquerque, New Mexico, USA

O. Buluy
N. Aryasova
Yu. Reznikov
Institute of Physics of National Academy of Science,
Prospect Nauki, Kyiv, Ukraine

Ion Beam alignment of nematic liquid crystal on the surface of poly[2-methoxy-5-(2-ethylhexyloxy)-1,4-phenylenevinylene] was studied. Our results demonstrate that ion beam treatment provides uniform alignment of LC at the polymer surface, which is characterized by a weak anchoring. Application of polarization microscopy, magneto-optical measurements, Confocal Microscopy and X-ray Photoelectron Spectroscopy, allows us to propose a model of ion beam alignment. Oblique ion bombardment results in an angular anisotropic destruction of side chains and conjugated fragments of the polymer. This results in anisotropic angular distribution of polymer fragments, producing an axis of easy orientation for LC in the direction parallel to the projection of the ion beam.

Keywords: Confocal Microscopy; ion beam alignment; MEH-PPV; nematic liquid crystal; XPS

1. INTRODUCTION

The development of LCD technologies requires homogeneous alignment of liquid crystals (LCs). The traditional rubbing technique, consisting of

This work is supported by NSF CHE-9613880 and by CRDF grant UK-P1-2598-KV-04. The XPS was funded by a grant from the Keck Foundation and NSF CHE-0113724. Confocal Microscopy is funded through UNM Keck Nanofluidics Laboratory.

Address correspondence to Yuri Reznikov, Institute of Physics of National Academy of Science, Prospect Nauki 46, Kyiv 03028, Ukraine. E-mail: yuri@iop.kiev.ua

unidirectional brushing of the aligning substrates is quite reliable and provides good anchoring characteristics but has some drawbacks, including the production of electrostatic charges and introduction of dust during the rubbing. In addition, the traditional rubbing technique does not allow effective control of direction of the easy orientation axis and other anchoring parameters. Ion and plasma-beam alignment are among the more promising candidates to replace the rubbing procedure [1–7]. A variety of materials, including polyimides, ITO-electrodes, glass, diamond-like carbon, and polystyrenes can serve as effective alignment layers after ion beam treatment.

Here we report a study of ion beam alignment on the surface of a poly(*p*-phenylene-vinylene), PPV, derivative. The PPV-based materials are conjugated polymers that are widely used in organic light emitting devices (OLEDs) as effective electroluminescence emitters [8,9]. The potential combination of the emitting and aligning material in one layer offers the potential for development of new LC-OLE systems [10].

2. MATERIALS AND SAMPLES PREPARATION

We studied the ion beam-induced alignment of the nematic LC pentyl-cyanobiphenyl (5CB) from Merck on a surface of poly[2-methoxy-5-(2-ethylhexyloxy)-1,4-phenylenevinylene] (MEH-PPV) from Sigma-Aldrich. The average molecular weight of the polymer was 150,000–250,000. A thin film of MEH-PPV was spin-coated or solvent-cast on an ITO glass substrate from a tetrahydrofuran or toluene solution with concentration less than 1% by weight. Polyimide, PI 2555, from Dupont, was used as a reference material. The polyimide films were deposited on the ITO glass by spin-coating a solution of polyamic acid on to the substrate, followed by soft-baking at 90°C for 1 min and hard-baking at 250°C for 1 hour.

The polymer films were bombarded with a 2 keV Ar ion beam at a 45° angle to the surface plane. The Ar^+ ion gun on the Kratos AXIS Ultra photoelectron spectrometer was used as the argon beam source. Two speeds, fast and slow, of ion beam rastering during bombardment are available in the instrumental setup.

3. RESULTS AND DISCUSSION

General Characterization of Ion Beam Alignment

The general characterization of the alignment was carried out by traditional polarization microscopy. We used combined cells, consisting of a test substrate covered with MEH-PPV and a reference substrate covered with rubbed polyimide film, to evaluate the alignment quality and orientation. The resulting LC textures were observed using a polarizing microscope. The angle, φ_0, between rubbing direction on the reference surface, d_{ref}, and projection of the ion beam on the test surface, d_{test}, was 45°. The reference substrate provided a strong anchoring of 5CB with a small pretilt ($<1.5^\circ$). The thickness of the cells was set by 50 μm rod-spacers.

The cells were filled with liquid crystal 5CB at 30°C. The clear, nematic phase, LC became discolored during capillary-effect based cell filling at room temperature, indicating partial dissolution of the MEH-PPV. LC emptied from the cell was observed to be orange in color, further verifying this observation. To test if there was a difference between the interaction of LC and polymer in bombarded versus unbombarded areas, we refilled the cell with fresh LC. The areas of the cell containing unbombarded polymer were colorless, while the bombarded areas retained the light orange color characteristic of MEH-PPV. The subsequent removal of the LC from the cell showed no additional color changes in the 5CB. These simple experiments demonstrated that the MEH-PPV is dissolved by 5CB in the unbombarded areas, while the bombarded polymer layer is more stable.

Analysis of the LC textures in the combined cells showed that relatively homogeneous planar structures are present in unbombarded areas and twist structures are observed in the bombarded areas. The twist angle, φ_{test}, in the bombarded areas was in a range of 35°–43°. Thus, the orientation of the LC is defined by the reference substrate in unbombarded areas. With respect to the bombarded areas, it is reasonable to suppose that the director is oriented along the projection of the ion beam at the surface. This conclusion follows from the fact that φ_{test} is close to the angle of ion beam incidence, $\varphi_0 = 45^\circ$. A deviation of φ_{test} from φ_0 is caused by the relatively weak anchoring of the LC on the tested surface. The ion beam alignment did turn out to be rather stable; we did not find visible changes in the twist in 30 days. Besides, the alignment in the irradiated areas preserved after the heating of the cell above clear point and refilling by a fresh LC (we observed some deterioration of the alignment in this case).

Anchoring Energy Measurements

In order to determine the anchoring energy of LC, W, on bombarded and unbombarded MEH-PPV surfaces we used the magneto-optics technique, recently proposed by Andrienko [11] and Faetti [12]. This technique is based on measurements of the reorientation of the LC director over the tested surface of the combined cell as a function of the magnetic field $\vec{H}$, followed by fitting of the experimental data with the analytical expressions for the reorientation angle, $\phi_{test}(\vec{H})$. In our experiments, the combined cells were placed between the magnet poles so that the direction $\vec{H}$ was parallel to the direction d_{ref}. If the director on the tested surface, $\vec{d}_{test}$ is not parallel to $\vec{d}_{ref}$ (as in this case), the magnetically-induced torque causes reorientation of the director in the bulk and on the tested surface toward d_{ref}, and the reorientation angle depends on the anchoring energy, W_{test}. The cell was tested by the probe He-Ne laser beam directed from the side of the reference surface and the polarization of the beam was parallel to $\vec{d}_{ref}$. Rotating the analyzer direction corresponding to the intensity maximum was measured. Using the Berreman matrix approach [13] director orientation at the tested surface φ_{test} was determined.

Balancing the torques at the tested surface gives:

$$-\frac{\sin\phi_{test}}{\xi_H} = \frac{W_{test}}{2K_{22}}\sin 2(\phi_{test} - \phi_0), \tag{1}$$

where $\xi_H = \sqrt{K_{22}/\chi_a}(1/H)$ is the magnetic coherence length, and ϕ_0 is the direction of the easy axes on the tested surface.

The dependencies of the twist angle vs. magnetic field for $\phi_0 = 45^\circ$ are shown in Figure 1. The increase in the anchoring energy of the LC on the IB bombarded polymer surface with increase of exposure time was detected. Calculated anchoring energy on the polymer bombarded for 15 sec using fast mode was $(5.7 \pm 1.2)*10^{-3}$erg/cm^2, while after 45 sec of bombardment using the same mode the value of anchoring energy increased to $(2.1 \pm 1.2)*10^{-2}$ erg/cm^2. The measured value of the anchoring energy appeared to be slightly less than the typical value produced by plasma/ion-alignment [7]. The measured values of the anchoring energy did not change within 60 days.

The anchoring energy measured in the unbombarded area is $3*10^{-3}$ erg/cm^2 and about one order lower than in the bombarded area, indicating less strong physico-chemical interactions between LC molecules and unbombarded MEH-PPV. We found a decrease of the anchoring energy in the unbombarded area to 10^{-4} erg/cm^2 after 60 days from the first measurements. We associate this phenomenon with gradual dissolution of the MEH-PPV layer in the LC.

XPS Surface Analysis

To study how ion beam bombardment changes the chemical composition of MEH-PPV surfaces we used XPS surface analysis. Analyses were performed using the Kratos Axis Ultra X-ray photoelectron

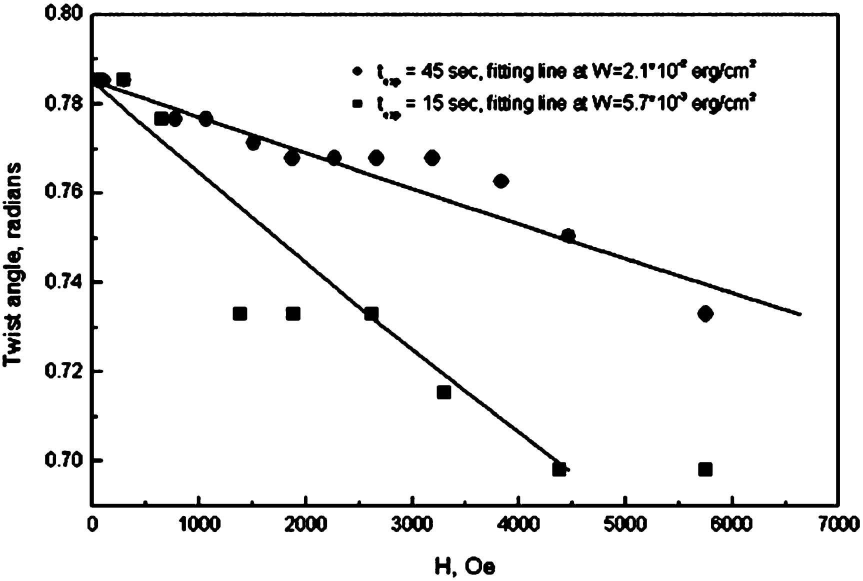

FIGURE 1 Dependence of the twist angle, ϕ_{test} on the magnetic field for t_{exp} =15 min (■) and t_{exp} =45 min (•). The fitting according (1) gives W(15s) = 5.7×10^{-3} erg/cm^2 and W(45s) = 2.1×10^{-2} erg/cm^2.

spectrometer with a monochromatic Al K$\bar{\alpha}$ source operating at 300 W. Samples for XPS analysis were IB bombarded for 15, 30, 60 and 120 seconds using the slow speed of ion rastering. Low resolution wide scan and high-resolution spectra (C 1s, O 1s and N 1s for polyimide and C 1s and O 1s for MEH-PPV) were acquired at pass energies of 80 eV and 20 eV, respectively.

Curve-fits of high-resolution C 1s spectra were used to evaluate the chemical composition of unbombarded and bombarded MEH-PPV films [14,15]. The C 1s spectra were curve-fit using 5 peaks at binding energies of 284.6, 285, 286.35, 288.3 and 291.7 eV, identified as C=C, C–C and/or C–H, C–O, C=O, and O–C=O respectfully (Fig. 2). Changes in the C 1s spectra provide information about variations in chemical composition as a result of ion bombardment (compare Figs. 2a and 2b and Table 1). In contrast to our previous results [5], where ion beam alignment of polyimides and polystyrene was explored, 2 minutes of bombardment did not significantly change the concentration of carbon atoms in the phenyl rings. We did observe, however, a reduction in the number of C–O bonds (Fig. 2b), located in the side-chains of the polymer structure. The depletion of these fragments was confirmed by elemental quantification of the survey

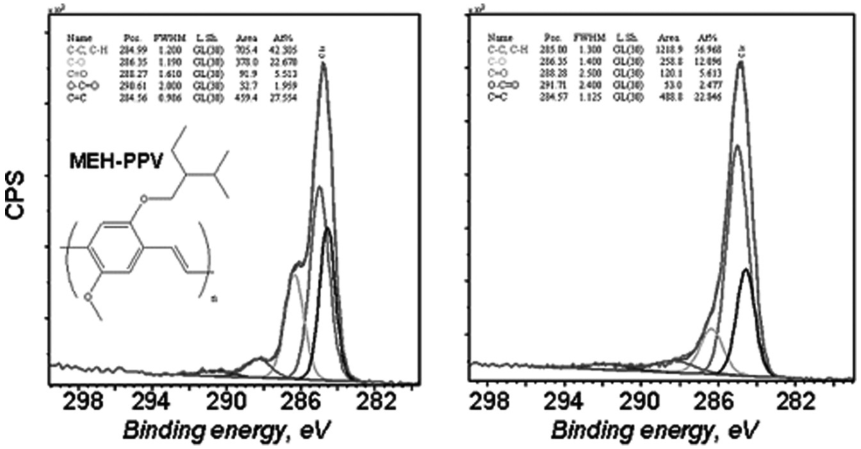

Name	Pos.	FWHM	L.Sh.	Area	At%
C-C, C-H	284.99	1.200	GL(30)	705.4	42.305
C-O	286.35	1.190	GL(30)	378.0	22.670
C=O	288.27	1.610	GL(30)	91.9	5.513
O-C=O	290.61	2.000	GL(30)	32.7	1.959
C=C	284.56	0.906	GL(30)	459.4	27.554

Name	Pos.	FWHM	L.Sh.	Area	At%
C-C, C-H	285.00	1.300	GL(30)	1218.9	56.968
C-O	286.35	1.400	GL(30)	258.8	12.096
C=O	288.28	2.500	GL(30)	120.1	5.613
O-C=O	291.71	2.400	GL(30)	53.0	2.477
C=C	284.57	1.125	GL(30)	488.8	22.846

FIGURE 2 High-resolution C 1s spectra of MEH-PPV a) $t_{exp} = 0$; b) $t_{exp} = 2$ min. Insert shows the chemical structure of MEH-PPV.

spectra and curve fitting of the O 1s high-resolution spectra. Therefore, it is reasonable to suggest that the mechanism of alignment on the surface of the MEH-PPV at short bombardment times is caused by anisotropic depletion of the side chain C–O bonds. Side chains are known to increase solubility of PPV in organics [16,17]. Destruction of C–O bonds in side chains decreases the polarity of the polymer, and can be a reason for the decreased solubility of MEH-PPV in 5CB after ion bombardment.

Multispectral Fluorescence Confocal Microscopy

Multispectral confocal imaging provides a powerful tool for the analysis of polymeric materials containing fluorophores with very close or

TABLE 1 Quantification of C 1s High-Resolution Spectra of MEH-PPV as a Function of Bombardment Time

Concentration, %	Unbomb	IB 15 sec	IB 30 sec	IB 60 sec	IB 120 sec	% Change, IB 2 min
Phenyl	27.6	28.5	24.9	24.4	22.8	–17.1
Alkyl	42.3	43.9	47.1	52.1	57.0	34.7
C–O	22.7	20.1	20.0	15.4	12.1	–46.6
C=O	5.5	5.6	6.5	6.0	5.6	
O–C=O	2.0	2.0	1.4	2.0	2.5	

even overlapping emission spectra [18,19]. In this study, we used confocal imaging to further investigate the effects of ion bombardment on the chemical composition and morphology of MEH-PPV. Measurements were made using a LSM 510 META Axiovert 200 confocal microscope (Carl Zeiss, Germany) to detect the surface fluorescence spectra induced by an Ar^+ ion laser ($\lambda = 488\,nm$). Fluorescence images at 24 spectral channels from 494 to 740 nm, with a spectral width of 10.7 nm, were acquired.

We obtained the fluorescence spectral images of the MEH-PPV surfaces for $t_{exp} = 0, 2, 5, 7$, and 10 minutes of bombardment time. The images were acquired at the same microscope settings of so that they can be compared quantitatively. In addition, a copper grid (Ted Pellar Inc.) with 120 micron spacing was placed on one of MEH-PPV films, and this sample was bombarded by the ion beam for 2 minutes. Figure 3 shows confocal images acquired at the maximum wavelength of emission, λ_{max}, from unbombarded MEH-PPV, from the sample bombarded for $t_{exp} = 5\,min$ and for the sample bombarded through the grid for $t_{exp} = 2\,min$. The images obtained for $t_{exp} = 2, 7$, and 10 min looked similar to the image of $t_{exp} = 5\,min$. The image of the unbombarded sample is featureless and has less fluorescence intensity then the image from the ion-bombarded sample. In addition, the ion-bombarded samples reveal evident anisotropic micro-relief patterns. Elongated features increase in length as the time of bombardment increases to $t_{exp} = 7\,min$, while at 10 minutes the roughness of the surface decreases. The enhancement of MEH-PPV fluorescence by the IB is also confirmed by the sample bombarded through the grid from a comparison of the brighter bombarded and darker unbombarded areas.

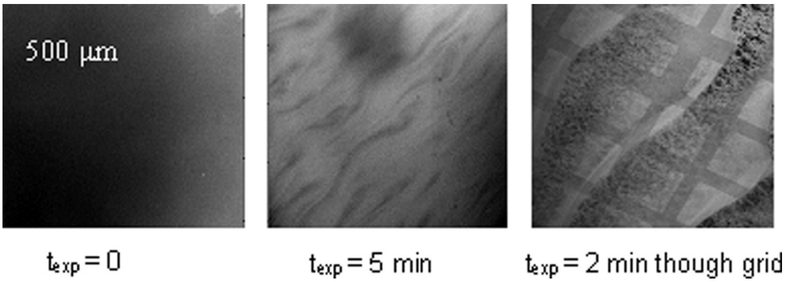

FIGURE 3 Fluorescence image at λ_{max} for unbombarded, IB-bombarded for 5 minutes and IB-bombarded for 2 minutes through gird. IB increases fluorescence intensity of PPV. The anisotropic micro-relief pattern is created by IB modification.

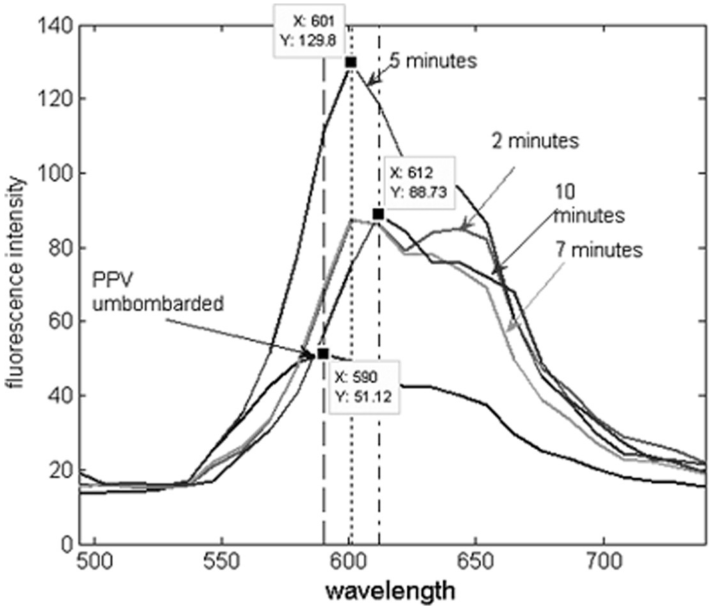

FIGURE 4 Spectral profiles from the images shown in Figure 4. Red shift is observed as a result of IB exposure. The intensity increases with time of bombardment as a result of formation of large conjugated structure and then decreases as the conjugated structure is destroyed at further times of bombardment.

Figure 4 shows the dependence of the fluorescence spectra on the bombardment time. The maximum of emission, $\lambda_{\max}$, for the unbombarded sample is at 590 nm. The fluorescence intensity initially increases with time of ion bombardment and then decreases at longer times. In addition, a shift of $\lambda_{\max}$ to longer wavelength of 601 nm is observed. This red shift, and concurrent increase of fluorescence intensity, in the ion beam bombarded samples may be due to stronger π-π interactions between the conjugated units and, potentially, a larger conjugated structure [20]. We associate this enhancement of π-π interactions with partial removal of side chains, clearly detected by XPS analysis above. Removal of a part of side fragments results in a decrease of the shielding effect due to the side chains.

The observed decrease of fluorescence intensity at long bombardment can be associated with the destruction of the conjugated structures. The observed smoothing of the bombarded surface at long exposures also points at significant destruction of polymeric structure.

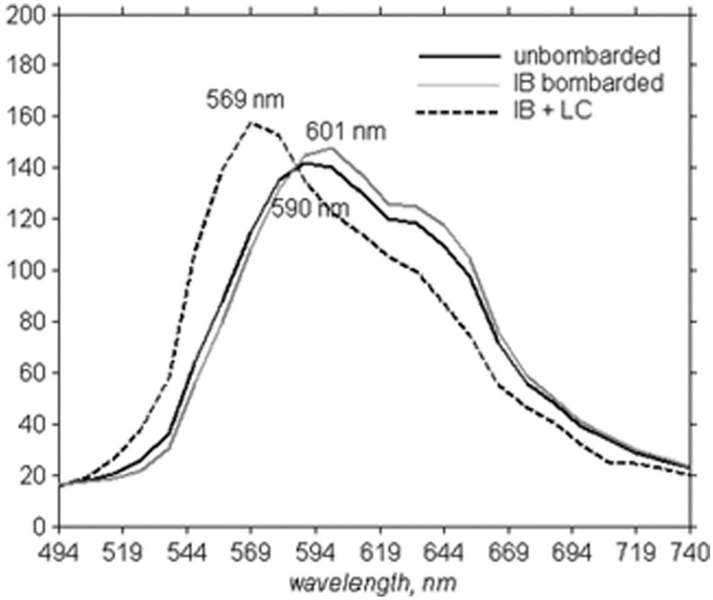

FIGURE 5 Spectral profiles extracted from area bombarded to IB, unbombarded and from IB MEH-PPV with LC on top. IB causes red shift, while interaction of PPV with LC causes large blue shift.

After the confocal analysis was performed on the MEH-PPV sample bombarded through the grid, LC was spin coated onto its surface. We found an apparent enhancement of the quantum efficiency of MEH-PPV in this case. A comparison of the spectra from bombarded and unbombarded areas of MEH-PPV (Figure 5) shows a small but detectable red shift in the bombarded area, consistent with Figure 4. A distinctive feature of the spectra of MEH-PPV covered with LC is a large blue shift in the MEH-PPV spectrum. This blue shift is caused a sharp decrease of interchain interactions between MEH-PPV molecules at dissolution of the polymer in the LC [21].

4. CONCLUSIONS

Our results demonstrate that ion beam treatment provides uniform alignment of LC along the projection of ion beam at the MEH-PPV surface. The measurements of the anchoring energy by magneto-optics technique shows rather weak anchoring values, $W \sim (10^{-2}–10^{-3})\,\mathrm{erg\,cm^{-3}}$. Application of multiple techniques (polarization microscopy, magneto-optical measurements, multispectral confocal microscopy and X-ray photoelectron spectroscopy) allows us to propose a tentative mechanism of ion beam alignment. Oblique ion bombardment results in an angular anisotropic destruction of the polymer due to breaking side chains and conjugated fragments. Because of different probability of the destruction, the break of side chains prevails at the short exposure and the destruction of the conjugated system in the main chain occurs at the long exposure time. Both processes result in anisotropic angular distribution of initial and modified polymer fragments, and in turn, in producing the axis of easy orientation for LC parallel to the projection of the ion beam on the surface plane. As the destruction of the polymer results in a decrease of the polarity of the surface, it becomes more stable leading to the decrease of MEH-PPV solubility in LC. Moreover, the bombardment smoothes the surface morphology that promotes the homogeneous alignment of LC.

REFERENCES

[1] Chaudhari, P., Lacey, J. A., Lien, S. A., & Speidell, J. L. (1998). *Jpn. J. Appl. Phys.*, *37*, L55.

[2] Chaudhari, P., Lacey, J. A., Doyle, J., Galligan, E., Lien, S. A., Callegari, A., Hougham, G., Lang, N. D., Andry, P. S., John, R., Yang, K. H., Lu, M. H., Cai, C., Speidell, J., Purushothaman, S., Ritsko, J., Samant, M., Stohr, J., Nakagawa, Y., Katoh, Y., Saitoh, Y., Sakai, K., Satoh, H., Odahara, S., Nakano, H., Nakagaki, J., & Shiota, Y. (2001). *Nature* (London), *441*, 56.

[3] Stohr, J., Samant, M. G., Luning, J., Callegari, A. C., Chaudhari, P., Doyle, J. P., Lacey, J. A., Lien, S. A., Purushothaman, S., & Speidell, J. L. (2001). *Science*, *292*, 2299.

[4] Doyle, J. P., Chaudhari, P., Lacey, J. L., Galligan, E. A., Lien, S. C., Callegari, A. C., Lang, N. D., Lu, M., Nakagawa, Y., Nakano, H., Okazaki, N., Odahara, S., Katoh, Y., Saitoh, Y., Sakai, K., Satoh, H., & Shiota, Y. (2003). *Nuc. Instrum. Methods*, *206*, 467.

[5] Fulghum, J. E., Su, L. L., Artyushkova, K., West, J. L., & Reznikov, Y. (2004). *Mol. Cryst. Liq. Cryst.*, *412*, 1971.

[6] Yaroshchuk, O., Zakrevskyy, Yu., Dobrovolskyy, A., & Pavlov, S. (2001). *Proc. SPIE*, *4418*, 49.

[7] Yaroshchuk, O., Kravchuk, R., Dobrovolskyy, A., Qiu, L., & Lavrentovich, O. D. (2004). *Liq. Cryst.*, *31*, 859.

[8] Burroughes, J. H., Bradley, D. D. C., Brown, A. R., Marks, R. N., Mackay, K., Friend, R. H., Burns, P. L., & Holmes, A. B. (1990). *Nature* (London), *347*, 539.

[9] Jandke, M., Strohriegl, P., Gmeiner, J., Brutting, W., & Schwoerer, M. (1999). *Advanced Materials*, *11*, 1518.

[10] Weder, C., Sarwa, C., Montali, A., Bastiaansen, G., & Smith, P. (1998). *Science*, *279*, 835.

[11] Andrienko, D., Dyadyusha, A., Iljin, A., Kurioz, Yu., & Reznikov, Yu. (1998). *Mol. Cryst. Liq. Cryst.*, *321*, 271.

[12] Faetti, S. & Mutinati, G. C. (2003). *Phys. Rev. E*, *68*, 026601.

[13] Berreman, D. W. (1972). *J. Opt. Soc. Am.*, *62*, 502.

[14] Moulder, J. F., Stickle, W. F., Sobol, P. E., & Bomben, K. D. (1992). *Handbook of X-Ray Photoelectron Spectroscopy*, Physical Electronics Inc.: Eden Prairie.

[15] Briggs, D. & Grant, J. T. (2003). *Surface Analysis by Auger and X-ray Photoelectron Spectroscopy*, IM publications and Surface Spectra Limited: Chichester, Manchester.

[16] Wang, H. M., Tao, X. M., & Newton, E. (2004). *Polymer International*, *53*, 20.

[17] Zhu, Z. G. & Swager, T. M. (2002). *J. Am. Chem. Soc.*, *124*, 9670.

[18] Haraguchi, T., Shimi, T., Koujin, T., Hashiguchi, N., & Hiraoka, Y. (2002). *Genes to Cells*, *7*, 881.

[19] Stimson, M. J., Haralampus-Grynaviski, N., & Simon, J. D. (1999). *Rev. Sci. Instrum.*, *70*, 3351.

[20] Atreya, M., Li, S., Kang, E. T., Neoh, K. G., Ma, Z. H., Tan, K. L., & Huang, W. (1999). *Polymer degradation and Stability*, *65*, 287.

[21] Fritz, K. P. & Scholes, G. D. (2003). *J. Phys. Chem.*, *107*, 10141.